



HAL
open science

Rupture directivity of microearthquake sequences near Parkfield, California

Olivier Lengliné, Jean-Luc Got

► **To cite this version:**

Olivier Lengliné, Jean-Luc Got. Rupture directivity of microearthquake sequences near Parkfield, California. *Geophysical Research Letters*, American Geophysical Union, 2011, 38, pp.L08310. 10.1029/2011GL047303 . insu-00680902

HAL Id: insu-00680902

<https://hal-insu.archives-ouvertes.fr/insu-00680902>

Submitted on 12 Mar 2021

HAL is a multi-disciplinary open access archive for the deposit and dissemination of scientific research documents, whether they are published or not. The documents may come from teaching and research institutions in France or abroad, or from public or private research centers.

L'archive ouverte pluridisciplinaire **HAL**, est destinée au dépôt et à la diffusion de documents scientifiques de niveau recherche, publiés ou non, émanant des établissements d'enseignement et de recherche français ou étrangers, des laboratoires publics ou privés.

Rupture directivity of microearthquake sequences near Parkfield, California

O. Lengliné¹ and J.-L. Got²

Received 2 March 2011; accepted 7 March 2011; published 29 April 2011.

[1] The direction of propagation is an important factor that affects the pattern of ground motion generated by an earthquake. Characterizing factors favoring a potential rupture propagation direction is thus an important task. Here we analyze the earthquake directivity of repeating earthquake sequences located on the San Andreas fault near Parkfield, California. All earthquakes of a sequence have very similar waveforms and have overlapping surface ruptures. We show that subtle variations of the transfer function between earthquakes of a common sequence can be interpreted as a change of apparent rupture duration. Relative apparent rupture durations are computed for all pairs of events at all available stations and for each sequence. We invert these measurements to obtain an estimation of the apparent rupture duration for each individual event of the sequence relative to a reference event. Variation of apparent rupture duration with azimuth attests for the rupture directivity. We show that the majority of analyzed microearthquakes presents a rupture in the south-east direction. We also show that, on a given repeating sequence, most earthquakes tend to show the same rupture direction. **Citation:** Lengliné, O., and J.-L. Got (2011), Rupture directivity of microearthquake sequences near Parkfield, California, *Geophys. Res. Lett.*, 38, L08310, doi:10.1029/2011GL047303.

1. Introduction

[2] Earthquake rupture is characterized, among other features, by its direction of propagation. This feature has important consequences in terms of potential damages as most of the energy will be carried out in the direction of rupture [e.g., *Boatwright*, 2007]. It is not yet clear which are the important parameters controlling the direction of rupture. As an example, the 1966 Parkfield earthquake has an inferred rupture propagation direction towards the south-east whereas the 2004 shock which ruptured the same fault patch propagated towards the north-west [*Bakun et al.*, 2005]. Numerical models of dynamic rupture suggest that material contrast across the fault plane might induce a preferential rupture direction [e.g., *Andrews and Ben-Zion*, 1997]. However there is still a lack of clear, direct, observational evidence of a statistical preferential rupture direction. Indeed, pre-stress on the fault plane is likely to be one of the factors controlling the rupture propagation direction. In order to uncover a preferential direction, one has to deal with a sufficient number of earthquakes to reduce the sta-

tistical noise induced by the effect of the pre-stress. Large earthquake datasets are mostly composed of low-magnitude events for which source characteristics are not accurately inferred. Here, we take advantage of repeating earthquake sequences previously isolated by *Lengliné and Marsan* [2009] to analyze the changes in directivity among earthquakes showing similar waveforms, and to provide a statistical evidence of factors controlling the rupture directivity. Similar attempts have been recently conducted by *Kane et al.* [2009] and E. Wang and A. M. Rubin (Rupture directivity of microearthquakes on the San Andreas fault from spectral ratio inversion, submitted to *Geophysical Journal International*, 2010). Repeating earthquake sequences used in this study have been identified based on (i) coherence criterion -coherence is a frequency dependent measure of similarity between waveforms-, (ii) nearly similar event magnitude and (iii) superposition of the source areas. The high number of events allows us to investigate the source process of multiple earthquake ruptures on the time span covered by the dataset (~22 years). Extracting significant information from these microearthquake sequences requires an adequate processing that makes use of the earthquake similarity. We employ a spectral ratio method which takes full advantage of the common ray paths of earthquakes of a common sequence to obtain precise estimates of their relative sources parameters. Despite the extreme similarity of the waveforms, small variations are observed and can be exploited in order to indicate changes in the source process. Such source parameters are extracted from an inversion procedure that is devoted to incorporate precise information concerning the various forms of uncertainties arising in our problem. This processing provides us with relative apparent durations with confidence intervals for each earthquake of a sequence. A simple model of rupture allows us to interpret our results in terms of propagation direction. Our study aims at i) analyzing whether earthquakes occurring at the same location always have the same directivity or not, ii) detecting whether microearthquakes in the Parkfield area show a statistical preferential rupture direction or not.

2. Data Processing

[3] We use 334 repeating sequences, identified by *Lengliné and Marsan* [2009], totaling 2414 earthquakes with magnitude ranging from $M_l = 1.0$ to 3.2. We follow the approach presented by *Got and Fréchet* [1993] to obtain the variation of rupture duration for a pair of earthquakes. We use 2.56 s-long P-wave records on the vertical component of short period stations of the Northern California Seismic Network (NCSN). All stations have a 100 Hz sampling frequency. We define N_{eq} as the number of earthquakes in the analyzed repeating sequence and n_{sta} the number of

¹IPGS, CNRS, Université de Strasbourg, Strasbourg, France.

²LGIT, CNRS, Université de Savoie, Le Bourget-du-Lac, France.

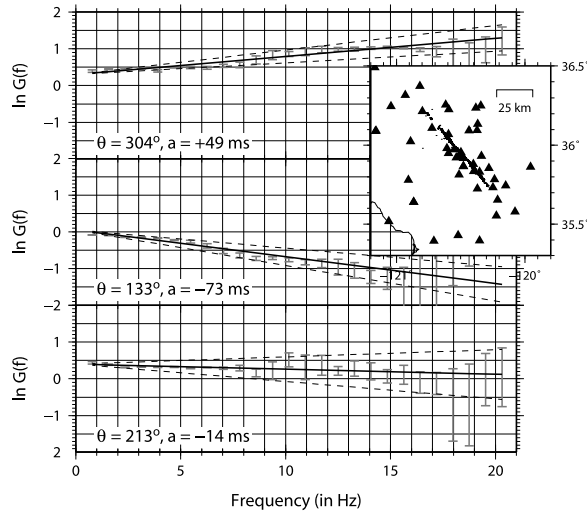


Figure 1. Variation of $\ln G$ as a function of the frequency (in Hertz) for a pair of earthquake at three different stations. The errorbars in gray denotes the values of $\ln G$ with their uncertainties (2σ confidence interval). The dark lines show the best linear fits and the dashed lines indicate the uncertainties, at the 2σ level, on the slope determination. The value of the slope, a , as well as the azimuth of each station relative to the doublet barycentre are shown in the bottom left corner for each station. The enclosed figure is a map centered on the studied area representing earthquakes used in this study (black dots) and stations which recorded at least 100 pairs of earthquakes (black triangles).

stations which recorded at least two earthquakes of this repeating sequence. We call $x_i^k(t)$ the record of the i th earthquake at station k ($i \in [1; N_{eq}]$ and $k \in [1; n_{sta}]$). For all n_{sta} stations we compute the modulus of the transfer function relating the Fourier transform of all possible pairs of events. This is the modulus of the Wiener filter existing between these two events. It is the least square estimate of what is often called the “spectral ratio” between two events. We call G_{ij}^k the modulus of this transfer function linking signals x_i^k and x_j^k . G_{ij}^k is computed at frequency, f , by

$$G_{ij}^k(f) = \frac{\overline{|X_i^k(f)X_j^{*k}(f)|}}{\overline{|X_i^k(f)X_i^{*k}(f)|} \overline{|X_j^k(f)X_j^{*k}(f)|}}, \quad (1)$$

where $X_i^k(f)$ is the Fourier transform of x_i^k , the star denotes the complex conjugate, $|z|$ is the modulus of z and the overbar designates smoothed quantity. The two signals are first iteratively aligned during the time-delay computation, using cross-spectral analysis. We used a 1.28 s-long Tukey tapering window; spectral densities are smoothed with the Fourier transform of a Hann window of order two. The order controls the smoothing width. The coherency, measuring the similarity between the two signals at a given frequency is given by

$$C_{ij}^k(f) = \frac{\overline{|X_i^k(f)X_j^{*k}(f)|}}{\sqrt{\overline{|X_i^k(f)X_i^{*k}(f)|}} \sqrt{\overline{|X_j^k(f)X_j^{*k}(f)|}}}. \quad (2)$$

A mean coherency, $\widehat{C}_{i,j}^k$, is computed between 3 and 20 Hz. The estimates of G_{ij}^k are kept when $\widehat{C}_{i,j}^k$ is larger than 90%.

3. Model

[4] Let us consider *Brune’s* [1970] f^2 source which describes the frequency content for a kinematic fault model. In such a model, the logarithm of the spectral ratio between two earthquakes with corner frequency f_{c1} and f_{c2} can be expressed as

$$\ln[G(f)] = \alpha + \ln \frac{1 + \left(\frac{f}{f_{c2}}\right)^2}{1 + \left(\frac{f}{f_{c1}}\right)^2}, \quad (3)$$

where α denotes the logarithm of the seismic moment ratio of the two events. We approximate the slope of $\ln(G)$ computed at $f=f_c$, where $f_c \simeq f_{c1} \simeq f_{c2}$ as earthquakes have nearly similar sizes, with the slope of $\ln(G)$ in the frequency range [3–20]Hz. This approximation is relevant as $\ln(G)$ is quasi-linear in the frequency range below f_c . Following *Got and Fréchet* [1993], the slope of $\ln(G)$ can be approximated at $f=f_c$ as $-\Delta f_c/f_c^2$, where $\Delta f_c = f_{c2} - f_{c1}$. Assuming $\tau \propto 1/f_c$, i.e., the rupture duration, τ , is inversely proportional to the corner frequency, we obtain that the slope of the logarithm of the spectral ratio is proportional to the variation of rupture duration. Therefore, taking the logarithm of $G_{ij}^k(f)$ and computing its slope with respect to frequency provides us with an estimate of the apparent variation of rupture duration between earthquakes i and j at station k . The slope of $\ln[G(f)]$ is computed with a simple least square fit where the uncertainty $\sigma_{ij}^k(f)$ on $\ln(G_{ij}^k(f))$ is approximated by the standard deviation of a Gaussian distribution, and with

$$\sigma_{ij}^k(f) = \begin{cases} \frac{1 - (C_{ij}^k(f))^2}{(C_{ij}^k(f))^2} & \text{if } C_{ij}^k(f) > 0.9 \\ \infty & \text{else} \end{cases} \quad (4)$$

we also impose $\sigma(f)$ to never be lower than 0.005 (equivalent to $C_{ij}^k(f) > 0.9975$) in order to not set unrealistically small uncertainties in the case of very coherent waveforms. The slope of $\ln(G_{ij}^k(f))$ is denoted a_{ij}^k and its uncertainty is $\sigma_{a,ij}^k$. We show in Figure 1 the typical variation of $\ln(G(f))$ for a pair of earthquakes at three different stations. We observe a clear linear decay whose fit provides values of a . It demonstrates that although waveforms are very similar, variations exist among them and can be analyzed.

[5] For all possible pairs of earthquakes at all possible stations, we use this method to obtain estimates of the variation of rupture duration. As we have measurements for all possible pairs, and all measurements have to be coherent between them, we can write a system of linear equations in order to estimate the apparent rupture duration $\Delta\tau_i^k$ for all events relative to the first event of the sequence. The problem we need to solve is linear and can be written as

$$\mathbf{d} = \mathbf{Gm}. \quad (5)$$

The data vector, \mathbf{d} , is composed by a_{ij}^k values. The parameter vector, \mathbf{m} , is made up of the τ_i^k values which are the

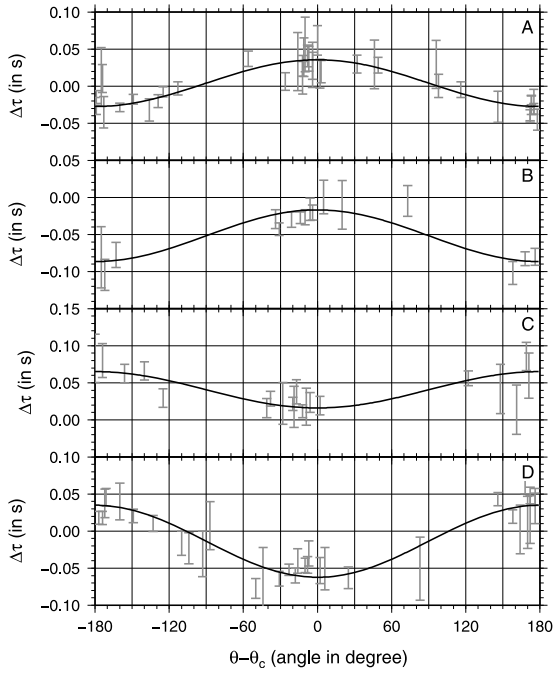


Figure 2. Variation of apparent rupture duration, $\Delta\tau_i^k$ as a function of the azimuth $\theta - \theta_c$ for several earthquakes, for different sequences. The error bars in gray denote the 2σ confidence interval of $\Delta\tau_i^k$ and the dark curve is the best cosine fit. We distinguish the 4 cases A–D. In cases A and D, values of $\Delta\tau$ are both positive and negative and thus correspond to the model presented in (10). For cases B and C, values of $\Delta\tau_i^k$ are either entirely positive or entirely negative and which corresponds to the model represented by equation (9).

apparent rupture duration of event i at station k that we want to determine. As $a_{ij}^k = \tau_j^k - \tau_i^k$, the Jacobian matrix \mathbf{G} only comprises 0, +1 and -1. Solution to equation (5) is provided by

$$\tilde{\mathbf{m}} = (\mathbf{G}^t \mathbf{C}_D^{-1} \mathbf{G} + \mathbf{C}_M^{-1})^{-1} (\mathbf{G}^t \mathbf{C}_D^{-1} \mathbf{d}_{obs} + \mathbf{C}_M^{-1} \mathbf{m}_{prior}), \quad (6)$$

where $\tilde{\mathbf{m}}$ is the *a posteriori* parameter vector and \mathbf{m}_{prior} is the *a priori* parameter vector, \mathbf{G}^t is the transpose of \mathbf{G} [Tarantola, 2005]. The data covariance matrix is \mathbf{C}_D and the *a priori* model covariance matrix is \mathbf{C}_M . \mathbf{C}_D is non empty only on the main diagonal with all $\sigma_{a,ij}^k$ values. We assign an *a priori* parameter uncertainty of 1 s except for the first event for which we assign a very small *a priori* uncertainty. All *a priori* parameters are set to 0 s. By fixing a very small *a priori* uncertainty on $m_{prior}(1)$, we thus impose that $\tilde{m}(1) \sim 0$ and thus that all results will be relative to $m(1)$. The *a posteriori* uncertainties are obtained with

$$\tilde{\mathbf{C}}_M = (\mathbf{G}^t \mathbf{C}_D^{-1} \mathbf{G} + \mathbf{C}_M^{-1})^{-1}. \quad (7)$$

We finally obtain the apparent durations of rupture $\Delta\tau_i^k$ for each event of the processed sequence and for each available station. All these estimates are relative to the apparent duration of the first event of the sequence, chosen as the

reference event. In order to keep only well resolved relative rupture duration estimates we discard all *a posteriori* parameters with associated uncertainties greater than 0.05 s.

4. Results

[6] For a kinematic source model, with a rupture propagating horizontally at velocity v_r along the fault strike, the apparent rupture duration τ_r is given by Haskell [1964]

$$\tau_r = \frac{L}{v_r} \left(1 - \frac{v_r}{c} \sin \phi \cos \theta \right), \quad (8)$$

where c is the P -wave velocity, θ is the azimuth of the station relative to the rupture direction and ϕ is the take-off angle. The distance L corresponds to the distance over which the rupture propagates; L equals the total fault plane length in the case of a unilateral rupture. As we are dealing with relative measurements, our results comprise both source properties not only of the earthquake i , but also of the first earthquake of the sequence used as a reference. We make the hypothesis that the rupture velocity for two earthquakes of a same sequence is similar. We also suppose that the rupture process of both earthquakes takes place on a fault plane with the same orientation and the same rupture mechanism. This is suggested from the focal mechanisms of earthquakes in the area which are almost entirely strike-slip [Thurber *et al.*, 2006]. We define $\theta_c = 140^\circ$ as the azimuth of the San-Andreas fault at Parkfield in the south-east direction [Thurber *et al.*, 2006]. For each earthquake of a sequence we want to determine its direction of rupture. The rupture direction is defined here as the direction for which the rupture propagates over the longest distance. This distance is equal to the fault plane length in a purely unilateral rupture and might be as small as $L/2$ for a perfectly bilateral rupture. Two scenarios are considered: i) both earthquake i and the reference earthquake have the same rupture direction or ii) the two earthquakes have opposite rupture directions. From equation (8) and considering that the apparent rupture duration is the difference between the initiating phase and the last stopping phase we can compute the relative apparent rupture duration. Depending on the two proposed cases, the relative apparent rupture duration will be respectively

$$\Delta\tau_i^k = \frac{L_i - L_0}{v_r} \left(1 \pm \frac{v_r}{c} \sin \phi_i^k \cos \theta'^k \right), \quad (9)$$

$$\Delta\tau_i^k = \frac{L_i - L_0}{v_r} \pm \frac{L_i + L_0}{c} \sin \phi_i^k \cos \theta'^k, \quad (10)$$

where $\theta' = \theta - \theta_c$. The lengths L_i and L_0 represent the distance over which the rupture propagates for earthquake i and the reference earthquake respectively. Distinguishing whether the ruptures we are inferring are closer to the unilateral case than to the bilateral case would require comparing $L_i - L_0$ with the fault plane length. As this last measurement is not known precisely we do not differentiate between these two cases and only investigate the direction of rupture as defined previously. We fit the azimuthal variation of $\Delta\tau_i^k$ with a function of the form

$$\Delta\tau_i^k = A_i + B_i \cos(\theta'^k) \sin(\phi^k), \quad (11)$$

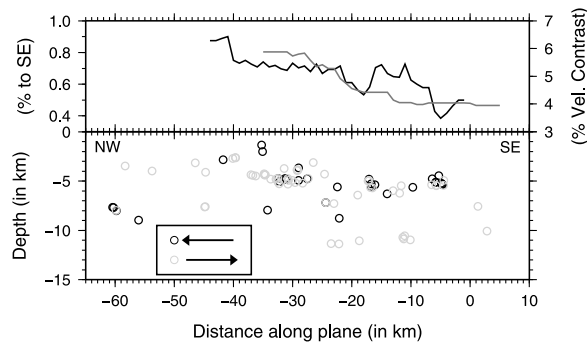


Figure 3. (bottom) Location of the 95 sequences, along the San Andreas fault plane, each of them showing at least one direction of rupture (gray circle: predominant rupture towards the south-east, black circle: towards the north-west). The horizontal axis is the distance along fault and its origin is defined as the hypocenter of the 2004, $M_w = 6$ mainshock. The vertical axis is the depth. (top) Proportion of sequences with a dominant rupture direction to the south-east (black). The proportion is computed from along strike bins of 10 km length when at least seven sequences fall into the considered bin. Average velocity contrast along the San Andreas fault plane from values by *Zhao et al.* [2010] (gray line).

where A_i and B_i are the parameters to be determined, σ_A and σ_B are their corresponding standard deviations. Such a function represents a valid fit for both scenarios (equations (9) and (10)). These two scenarios can be distinguished based on the signs of $\Delta\tau_i^k$ values. As $\frac{v_c}{c} < 1$, (equation (9)) shows that $\Delta\tau_i^k$ values may be positive or negative but can not be both. In this case, $|A| > |B|$ and both earthquakes (reference and tested earthquake) rupture propagates in the same direction. The rupture direction is obtained from the sign dependence of equation (9). Rupture propagates in the direction of θ_c if the sign is positive, in the opposite direction else. It results that the direction of rupture of the tested earthquake is given by the azimuth for which $|\Delta\tau_i^k|$ is minimum. When $|B| > |A|$, $\Delta\tau_i^k$ takes positive and negative values. The rupture direction of the event i is controlled by the sign dependence of equation (10) and thus by the sign of B . This rupture direction is given by the azimuth for which $\Delta\tau_i^k$ is minimum. We note that our two scenarios prescribed the rupture to occur in two directions only: on the direction of θ_c or opposite to it.

[7] The relative apparent rupture duration presents (Figure 2) a clear azimuthal pattern that is well fitted by the proposed cosine form (equation (11)). Our model (equations (9) and (10)) implies that the variation of $\Delta\tau$ with azimuth is solely explained by the difference in location of hypocenters, eventually leading to changes in rupture direction. We may wonder if any other possible change between the two earthquakes can also modify the proposed patterns. As proposed by *Got and Fréchet* [1993], we can first exclude a change of attenuation as it induces only a weak variation of $\Delta\tau$ compared to the one observed. These authors also showed that a change of rupture velocity or a change of focal mechanism due to local variations of the fault plane geometry will not produce a pattern similar to the one proposed (equations (9) or (10)) and thus will be discarded in the following analysis due to the resulting high misfit with equation (11).

[8] In order to avoid interpreting fits which are not well constrained and to reject ambiguous cases, we reject estimates of rupture direction when $\sigma_B > 5 \cdot 10^{-3} s$ and when $|B| < 2\sigma_B$. We finally obtain 95 sequences for which at least one rupture direction has been determined. These 95 sequences provided 273 estimates of rupture directions, 188 of which are in the direction of θ_c , i.e., to the southeast which represents 69% of all estimates. Restricting our analysis with sequences comprising at least 3 estimates of rupture direction, we find 35 sequences with a total of 197 rupture direction estimates, 135 of them (or 69%) being oriented toward the southeast. We can thus infer that microearthquakes in our dataset preferentially rupture in the southeast direction. We divided the 35 sequences, with at least 3 directivity estimates, based on the most abundant rupture direction of each sequence. We obtain 26 sequences with a dominant directivity towards the southeast and 9 sequences with a dominant directivity towards the north-west. We also investigate whether the direction of rupture varies for earthquakes in a common sequence or not. For the 35 sequences with at least 3 direction estimates, 84% of the ruptures on a sequence are found in the same direction. This suggests that earthquakes on an identified repeating source tend to have the same direction of rupture. We also show in Figure 3 the repartition along the fault plane of all the 95 sequences with their preferential rupture direction. We observe a decrease of the preferential direction of rupture towards the south-eastern bound of the fault segment.

5. Discussion and Conclusion

[9] Several mechanisms might be invoked in order to explain the preferential rupture direction of the earthquake towards the south-east. One of them involves material contrast across the fault plane. The rupture on such bimaterial interface is influenced by normal stress reduction in a favored direction which produces the directivity effect. Such a bimaterial model may represent an appropriate description of our studied zone. Indeed we analyze earthquake sequences located on the San Andreas fault which is supposed to mark an important material contrast [e.g., *Thurber et al.*, 2006; *Zhao et al.*, 2010]. Numerical models and theoretical studies suggest that the earthquake rupture directivity is preferentially oriented in the slip-direction of the less-rigid material (towards the south-east) [e.g., *Weertman*, 1980; *Andrews and Ben-Zion*, 1997; *Ben-Zion and Andrews*, 1998; *Cochard and Rice*, 2000; *Rubin and Ampuero*, 2007; *Ampuero and Ben-Zion*, 2008]. It has however been proposed by *Harris and Day* [2005] that the propagation direction might not be a direct consequence of the material contrast as pre-stress can also influence the rupture direction [e.g., *Andrews and Harris*, 2005; *Ampuero and Ben-Zion*, 2008] and bilateral rupture are also found in numerical rupture on bimaterial interface [*Harris and Day*, 1997]. A suggestion for a preferred rupture direction however comes from the observation of an asymmetric distribution of immediate aftershocks of microearthquakes on the San Andreas fault plane [*Rubin and Gillard*, 2000]. Our results indicate that microearthquakes in the Parkfield area statistically show a preferential rupture direction, i.e., a systematic tendency of the moment density distribution relative to the hypocenter to skew toward the southeast. Such an asymmetry has also been evidenced by *Wang and*

Rubin (submitted manuscript, 2010). Furthermore, this preferred direction of rupture is in agreement with the direction predicted from the velocity contrast across the fault plane. Our results are also supported by the progressive variation of the velocity contrast along the fault plane. As evidenced by *Thurber et al.* [2006] and *Zhao et al.* [2010] the material contrast is weaker towards the southeast portion of the fault segment near the 2004, mainshock location. We see on Figure 3 that this reduction of the velocity contrast, imaged by *Zhao et al.* [2010], closely follows the decrease of the proportion of earthquake sequences showing a preferential direction towards the south-east. Due to the averaging procedure used to estimate the velocity contrast, only the variation of the velocity contrast should be considered not the absolute values. Our findings suggest that material contrast across the fault plane is a possible cause inducing this statistical preferential rupture direction. This effect is revealed only after the analysis of a sufficient number of similar earthquakes. Other factors, as the variability of the pre-stress along the fault plane -which may randomly affect the rupture direction of an individual earthquake- are reduced by the statistical averaging. This is also evidenced at the scale of the asperity for sequences with a sufficient number of events. At this scale, we observe that earthquakes on a common asperity show a statistically preferential rupture direction. It suggests that, at the asperity scale as well, the rupture direction is influenced by material contrast and is also dependent on other effects as pre-stress at the source location. We note however that if the amplitude of stress heterogeneities is scale-dependent, the microearthquake observations presented in this study might be hard to extrapolate to large earthquakes.

[10] **Acknowledgments.** We thank the Northern California Seismic Network, U.S. Geological Survey, Menlo Park and the Berkeley Seismological Laboratory, University of California, Berkeley for providing the waveform data used in this study. We thank Peng Zhao and Zhigang Peng for sharing their values of the velocity contrast. This paper benefited from helpful comments of Alain Cochard and Luis Rivera and from useful reviews of Ruth Harris, Steven Day and Jean-Paul Ampuero.

[11] The Editor thanks Steven Day and an anonymous reviewer for their assistance in evaluating this paper. OL is supported by ANR grant SUPNAF.

References

- Ampuero, J.-P., and Y. Ben-Zion (2008), Cracks, pulses and macroscopic asymmetry of dynamic rupture on a bimaterial interface with velocity-weakening friction, *Geophys. J. Int.*, *173*, 674–692, doi:10.1111/j.1365-246X.2008.03736.x.
- Andrews, D. J., and Y. Ben-Zion (1997), Wrinkle-like slip pulse on a fault between different materials, *J. Geophys. Res.*, *102*, 553–571, doi:10.1029/96JB02856.
- Andrews, D. J., and R. A. Harris (2005), The wrinkle-like slip pulse is not important in earthquake dynamics, *Geophys. Res. Lett.*, *32*, L23303, doi:10.1029/2005GL023996.
- Bakun, W. H., et al. (2005), Implications for prediction and hazard assessment from the 2004 Parkfield earthquake, *Nature*, *437*, 969–974, doi:10.1038/nature04067.
- Ben-Zion, Y., and D. J. Andrews (1998), Properties and implications of dynamic rupture along a material interface, *Bull. Seismol. Soc. Am.*, *88* (4), 1085–1094.
- Boatwright, J. (2007), The persistence of directivity in small earthquakes, *Bull. Seismol. Soc. Am.*, *97*(6), 1850–1861, doi:10.1785/0120050228.
- Brune, J. N. (1970), Tectonic stress and the spectra of seismic shear waves from earthquakes, *J. Geophys. Res.*, *75*, 4997–5009, doi:10.1029/JB075i026p04997.
- Cochard, A., and J. R. Rice (2000), Fault rupture between dissimilar materials: Ill-posedness, regularization, and slip-pulse response, *J. Geophys. Res.*, *105*, 25,891–25,907, doi:10.1029/2000JB900230.
- Got, J.-L., and J. Fréchet (1993), Origins of amplitude variations in seismic doublets: Source or attenuation process?, *Geophys. J. Int.*, *114*, 325–340, doi:10.1111/j.1365-246X.1993.tb03921.x.
- Harris, R. A., and S. M. Day (1997), Effects of a low-velocity zone on a dynamic rupture, *Bull. Seismol. Soc. Am.*, *87*(5), 1267–1280.
- Harris, R. A., and S. M. Day (2005), Material contrast does not predict earthquake rupture propagation direction, *Geophys. Res. Lett.*, *32*, L23301, doi:10.1029/2005GL023941.
- Haskell, N. A. (1964), Total energy and energy spectral density of elastic wave radiation from propagating faults, *Bull. Seismol. Soc. Am.*, *54*(6A), 1811–1841.
- Kane, D. L., P. M. Shearer, B. Allmann, and F. L. Vernon (2009), Searching for evidence of a preferred rupture direction in small earthquakes at Parkfield, *Eos Trans. AGU*, *90*(52), Fall Meet. Suppl., Abstract S23B–1749.
- Lengliné, O., and D. Marsan (2009), Inferring the coseismic and postseismic stress changes caused by the 2004 $M_w = 6$ Parkfield earthquake from variations of recurrence times of microearthquakes, *J. Geophys. Res.*, *114*, B10303, doi:10.1029/2008JB006118.
- Rubin, A. M., and J.-P. Ampuero (2007), Aftershock asymmetry on a bimaterial interface, *J. Geophys. Res.*, *112*, B05307, doi:10.1029/2006JB004337.
- Rubin, A. M., and D. Gillard (2000), Aftershock asymmetry/rupture directivity among central San Andreas fault microearthquakes, *J. Geophys. Res.*, *105*, 19,095–19,109, doi:10.1029/2000JB900129.
- Tarantola, A. (2005), *Inverse Problem Theory and Methods for Model Parameter Estimation*, Soc. for Ind. and Appl. Math., Philadelphia, Pa.
- Thurber, C., H. Zhang, F. Waldhauser, J. Hardebeck, A. Michael, and D. Eberhart-Phillips (2006), Three-dimensional compressional wave-speed model, earthquake relocations, and focal mechanisms for the Parkfield, California, region, *Bull. Seismol. Soc. Am.*, *96*(4B), 38, doi:10.1785/0120050825.
- Weertman, J. (1980), Unstable slippage across a fault that separates elastic media of different elastic constants, *J. Geophys. Res.*, *85*, 1455–1461, doi:10.1029/JB085iB03p01455.
- Zhao, P., Z. Peng, Z. Shi, M. A. Lewis, and Y. Ben-Zion (2010), Variations of the velocity contrast and rupture properties of M6 earthquakes along the Parkfield section of the San Andreas fault, *Geophys. J. Int.*, *180*, 765–780, doi:10.1111/j.1365-246X.2009.04436.x.

J.-L. Got, LGIT, Université de Savoie, Campus Scientifique, F-73376 Le Bourget-du-Lac CEDEX, France. (jlgot@univ-savoie.fr)

O. Lengliné, IPGS, EOSt, Université de Strasbourg, 5 rue René Descartes, F-67084 Strasbourg CEDEX, France. (lengline@unistra.fr)